ACS Photonics

Letter

pubs.acs.org/journal/apchd5

Observation of Gate-Tunable Coherent Perfect Absorption of Terahertz Radiation in Graphene

Nurbek Kakenov,[†] Osman Balci,[†] Taylan Takan,[‡] Vedat Ali Ozkan,[‡] Hakan Altan,[‡] and Coskun Kocabas*[,†]

[†]Department of Physics, Bilkent University, 06800 Ankara, Turkey

[‡]Department of Physics, Middle East Technical University, 06800 Ankara, Turkey

Supporting Information

ABSTRACT: We report experimental observation of electrically tunable coherent perfect absorption (CPA) of terahertz (THz) radiation in graphene. We develop a reflection-type tunable THz cavity formed by a large-area graphene layer, a metallic reflective electrode, and an electrolytic medium in between. Ionic gating in the THz cavity allows us to tune the Fermi energy of graphene up to 1 eV and to achieve a critical coupling condition at 2.8 THz with absorption of 99%. With the enhanced THz absorption, we were able to measure the Fermi energy dependence of the transport scattering time of highly doped graphene. Furthermore, we demonstrate flexible active THz surfaces that yield large modulation in the THz reflectivity with low insertion losses. We anticipate that the gate-tunable CPA will lead to efficient active THz optoelectronics applications.

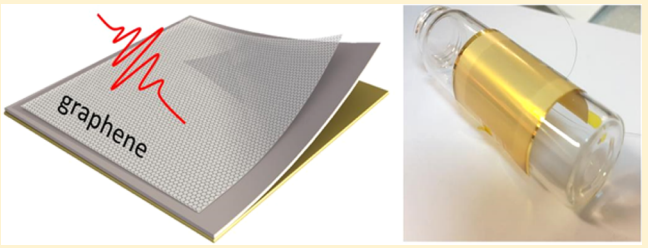

KEYWORDS: *graphene, coherent optical absorption, gate-tunable, terahertz, ionic gating, THz optoelectronics*

The phenomena of coherent perfect absorption (CPA) is the time-reversed analog of stimulated emission.[1−3] The optical absorption of a conducting thin film, which is limited to a maximum of 50% in freestanding form, can be enhanced under illumination of two coherent light beams when they are in-phase on the film. The concept of CPA has been implemented in various materials systems such as metamaterials,[4] two-level atomic systems,[5] phase change materials,[6] plasmonic systems,[7] and radar-absorbing surfaces.[8] Very recently the enhancement of optical absorption in two-dimensional conductors has attracted great attention for realization of gate-tunable optoelectronic devices. Enhancement of optical absorption in graphene, in particular, plays an important role in broadband tunable optoelectronic devices. The ability to control rates of interband[9−11] and intraband[12] electronic transitions via electrostatic gating enables novel active optoelectronic devices. At optical wavelengths, the optical absorption in graphene is limited to 2.3%;[10,11,13] however for longer wavelengths (THz[12,14,15] and microwave[8]) absorption can be increased up to 50% when the surface impedance of graphene (Z_G) matches half of the free space impedance,[16] $Z_G = 1/\sigma(\omega) = Z_0/2$ where Z_0 is the free space impedance and $\sigma(\omega)$ is the optical conductivity (see the small signal model given in Supporting Information Figure S1). To enhance the optical absorption further, various device structures have been explored. Patterning graphene into ribbons leads to enhanced absorption due to the localized plasmon oscillations. Fang et al. demonstrated absorption of 20% in far-IR frequencies.[17] Placing graphene on a photonic crystal cavity[18] or inside a microcavity[19,20] enhances the absorption due to multiple passes. Very recently, Thareja et al. placed graphene at a quarter-wave distance from a metallic surface and showed enhancement up to 5.5% in IR wavelengths.[21−23] With the help of local plasma frequency, complete optical absorption at IR frequencies has been proposed using periodically patterned doped graphene.[24,25]

Gate-tunable coherent absorption in graphene at terahertz frequencies has more technological importance because of being a low-cost alternative material for active THz devices. The recent theoretical studies show that gating graphene near a reflective surface would yield gate-tunable CPA for terahertz radiation.[26,27] They predicted that, under coherent illumination, 100% of THz radiation can be absorbed by a highly doped monolayer graphene when the Fermi energy is close to 1 eV. Varying the doping level, THz absorption can be controlled efficiently by electrical means. This is a challenging requirement. Although the static CPA in graphene for microwave[28] and visible[29,30] spectra has been reported, due to the limitation of conventional gating schemes, the gate-tunable CPA of THz radiation in graphene has not been observed yet.[12,31] In our previous works, we used ionic gating to control optical properties of graphene in a very broad spectrum extending from visible to microwave wavelengths.[8,13,14,32] In this Letter, we demonstrate a new type of tunable THz cavity that enables us to observe gate-tunable CPA. Figure 1a shows a schematic drawing of our device structure. The large-area monolayer

Received: April 6, 2016
Published: July 25, 2016

DOI: 10.1021/acsphotonics.6b00240
ACS Photonics 2016, 3, 1531−1535

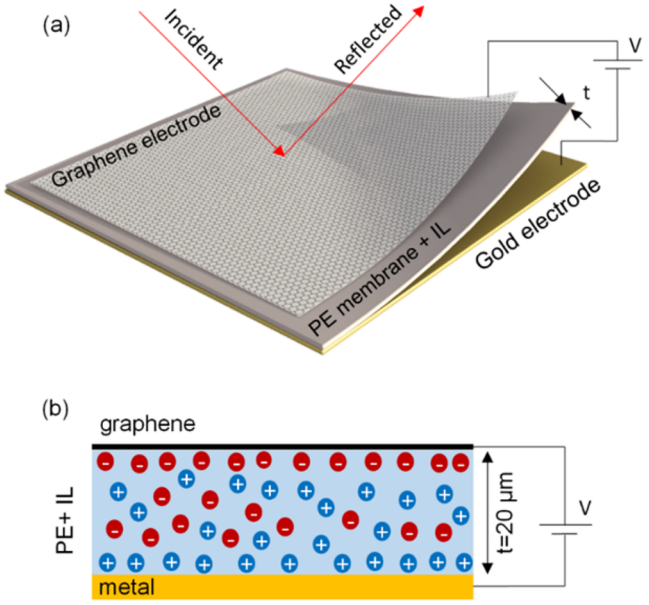

Figure 1. Active THz surfaces. (a) Schematic representation of electrically tunable THz cavity used for the coherent perfect absorption in graphene. The THz cavity is formed by a porous membrane sandwiched between graphene and gold electrodes. The thickness of the membrane is 20 μm. The ionic liquid electrolyte is soaked into the membrane. (b) Cross-sectional view of the cavity showing the formation of electrical double layers on the graphene and gold electrodes.

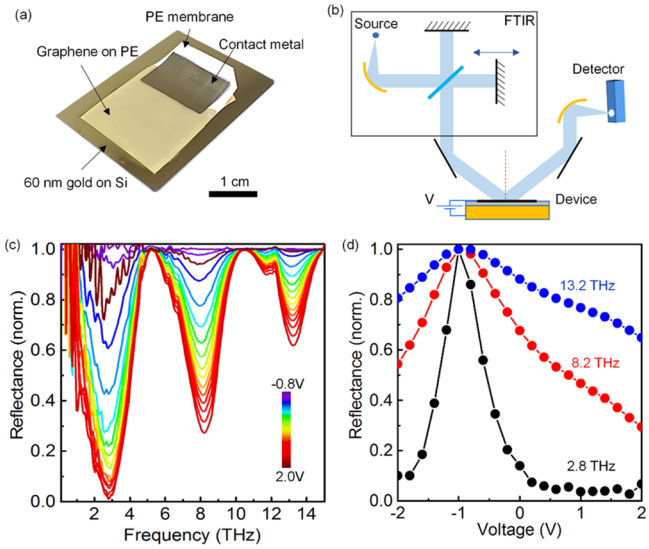

Figure 2. Coherent perfect absorption of THz radiation. (a) Photograph of the fabricated THz cavity. The monolayer graphene is transferred onto a PE membrane and placed on a gold-coated substrate. The 20-μm-thick membrane defines the cavity length, holds the electrolyte, and forms the mechanical support for graphene. (b) Experimental setup used for the THz measurements. (c) Reflectivity spectrum from the device at different bias voltages. (d) Variation of the resonance reflectance with gate voltage. The charge neutrality point is at −1 V.

graphene is synthesized by chemical vapor deposition on copper foils and then transferred onto a 20-μm-thick porous polyethylene membrane (42% porosity) that is placed on a reflective gold electrode. The thickness of the membrane defines the cavity length and the resonance wavelength. The gold electrode operates both as the back-reflecting mirror and the gate electrode. We soaked the membrane with room-temperature ionic liquid (diethylmethyl(2-methoxyethyl)-ammonium bis(trifluoromethylsulfonyl)imide, [deme][Tf2N]), which has a large electrochemical window that yields tunable Fermi energy on graphene up to 1 eV. Both the electrolyte and PE membrane are transparent between 0.1 and 15 THz (Supporting Information Figure S2). Figure 1b shows a schematic cross-sectional view of the device under a bias voltage that polarizes the ionic liquid in the membrane and forms electrical double layers (EDLs) near the graphene and gold interface. The EDL electrostatically dopes the graphene layer and alters its conductivity. Since the thickness of the EDL is very thin for ionic liquids, this configuration yields very large electric field and induced charges on the surface. The advantage of this device is that it provides a very efficient gating scheme with a charge density up to 10^{14} cm^{-2} and Fermi energy of 1 eV of the open graphene surface. These doping levels are enough to satisfy the CPA condition at THz frequencies. Our device yields a single-channel CPA when the incident and reflected THz beams are in phase at the graphene interface. For our device structure, the resonance condition can be written as $t\cos(\theta) = (2m + 1)\lambda/4n$ where θ is the incidence angle, t is the thickness of the membrane, m is an integer, and n is the index of refraction of the cavity. Spectroscopic measurements provide the resonances and antiresonances, which yield perfect and no absorption conditions, respectively.

Figure 2a shows the fabricated device. We measured THz reflection from the biased device using a Fourier transform infrared spectrometer (FTIR) equipped with a far-IR detector and a far-IR source (Figure 2b). Since ionic liquids have very low vapor pressure, we recorded the reflection spectrum under a vacuum (10 mTorr) to remove the absorption of water. Figure 2c shows the measured reflectivity spectrum from the device under different bias voltages. For a membrane thickness of 20 μm and incidence angle of 30°, we observed multiple resonance absorptions at 2.83, 8.24, and 13.23 THz frequencies. For the first resonance, we obtained an absorption of 99% at 2.0 V bias voltage. Unlike the condition of the freestanding film, CPA occurs when the real part of the optical conductivity of doped graphene reaches the values $\sigma(\omega) = 1/Z_0$ where Z_0 is the free space impedance. The optical conductivity of graphene at THz frequencies can be described with the Drude response as

$$\sigma(\omega) = \frac{e^2}{\pi\hbar}\frac{iE_F}{\omega + i\tau^{-1}}$$

where E_F is the Fermi energy and τ is the transport scattering time. For high doping levels, τ varies with the Fermi energy. We observed perfect absorption at low THz frequencies (<5 THz). For higher frequencies, however, the required doping levels exceed the accessible levels with the present device. The variation of the resonance reflectivity of the first three resonances is plotted in Figure 2d against the bias voltage. The reflectivity is normalized by the reflection at the charge neutrality point (CNP, around −1 V). The large shift in the CNP is associated with the work function difference between the graphene and gold electrodes. We obtained 99%, 76%, and 42% absorption for 2.83, 8.24, and 13.23 THz frequencies, respectively. To observe perfect absorption for higher order modes, we need larger voltages that exceed the electrochemical

DOI: 10.1021/acsphotonics.6b00240
ACS Photonics 2016, 3, 1531−1535

window of the electrolyte and introduce irreversible damage to the graphene electrode.

The Fermi energy provides a wealth of information about the electrical and optical properties of the device. Liu et al. predicted that, to achieve CPA in THz frequencies, the Fermi energy of graphene should be close to 1 eV, which yields the required optical conductance for the critical coupling. Near-IR and IR (see Supporting Information Figure S4) reflection spectra from the device provide direct measurement of the Fermi energy of the doped graphene. Figure 3a shows the

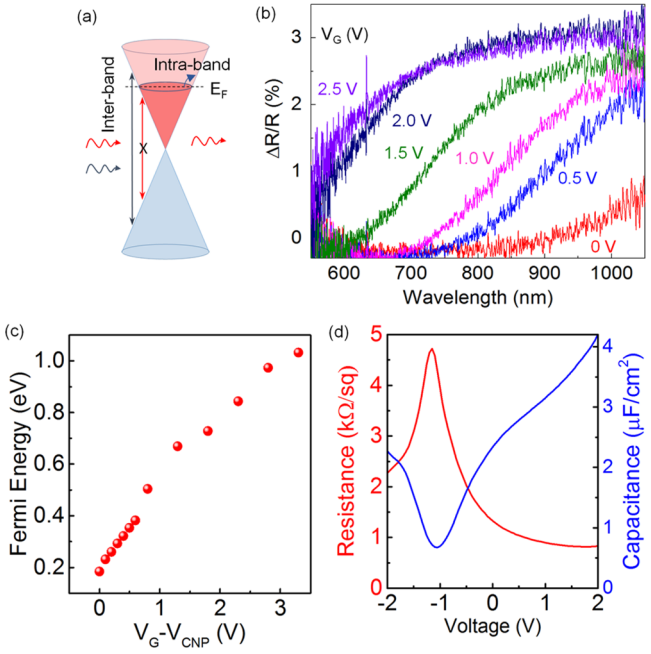

Figure 3. Electrical and optical characterization of the device. (a) Schematic representation of the band structure of graphene and possible electronic transitions. (b) Gate-tunable near-IR optical reflection from the graphene surface at different bias voltages. The number on the curves shows the bias voltage. (c) Fermi energy extracted from the reflection spectrum. (d) Variation of the resistance and capacitance of the devices with the bias voltage. At the charge neutrality point, resistance reaches a maxima of 4.5 kΩ and the capacitance goes to a minima of 0.8 μF/cm^2.

electronic band structure of doped graphene. Due to Pauli blocking, doped graphene has a gap in the optical absorption for photon energies $E < 2E_F$. Gating graphene results in an increase in the absorption gap and a step-like change in the reflectivity spectrum. Figure 3b shows the measured reflectivity spectra, which show a step-like change in the reflectivity with a cutoff wavelength at $2E_F$. Although monolayer graphene absorbs around 1.8% on a dielectric substrate, in our cavity structure, the reflectivity shows about 3% modulation due to multiple passes. Figure 3c shows the extracted Fermi energy as a function of bias voltage. At the charge neutrality point ($V_{CNP} = -1$ V) the unintentional doping level is 0.2 eV and increases linearly with a gate voltage up to 1 eV. At $V_G = 0$ V, graphene is significantly doped with a Fermi energy of 0.55 eV due to the work function difference between the gold and graphene electrodes. To get more insight, we performed electrical characterization of the device using an LRC meter. Figure 3d shows the variation of the resistance and capacitance of the devices with the bias voltage. At the charge neutrality point, the sheet resistance reaches 4.5 kΩ and decreases down to 0.8 kΩ, which also includes the contact resistance of the electrodes. The capacitance of the device shows a minima (0.8 μF/cm^2) at the charge neutrality point due to the minimum quantum capacitance of the graphene layer. The electrical characterization shows a good agreement with the spectroscopic measurements. Our results suggest that the critical coupling condition is achieved when the Fermi energy is around 1 eV.

The thickness of the porous substrates and the incidence angle define the frequency of the resonance absorption. We repeat our measurements with different membrane thicknesses. Figure 4 shows the gate-tunable reflectivity spectrum from two

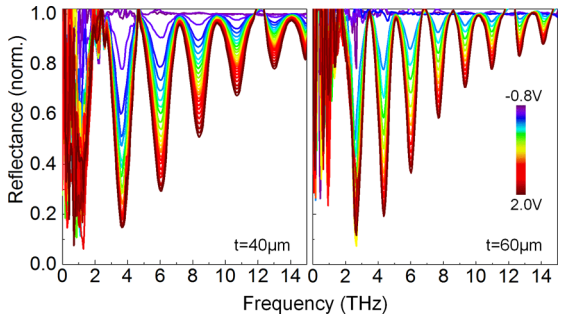

Figure 4. Tunable reflectivity from various THz cavities: Reflectance spectrum of THz cavities with 40 and 60 μm membrane thickness.

different devices with 40 and 60 μm cavity lengths. The observed resonance wavelengths satisfy the critical coupling condition as $\lambda_m = 4nt\cos(\theta)/(2m + 1)$. We do not observe a significant change in the frequency; however, the width of the resonance varies slightly with the bias voltage (see Supporting Information Figure S4). The fundamental resonances of the large cavities are buried under the noise level, due to the sensitivity of the FTIR system at low frequencies (<2 THz). We performed additional experiments using continuous wave tunable frequency THz sources (see Supporting Information Figure S5). Similarly, we obtained 98% modulation at 0.368 THz.

Recently, several THz pump−probe studies revealed semiconducting-to-metallic photoconductivity crossover in doped graphene.[33−35] These observations are due to the changes of the Drude weight and transport scattering time by the doping level. The enhanced optical absorption of graphene in the tunable THz cavity could provide a new platform to elucidate nonideal Drude responses of graphene at high doping levels. Due to the frequency dependence of the optical conductivity, the maximum absorbance decreases with frequency. By combining this frequency dependence with the direct measurement of the Fermi energy, we can extract the transport scattering time and its dependence on the Fermi energy. In Figure 5a, we plot the normalized resonance absorbance, which is proportional to the real part of the normalized optical conductivity, $\sigma(\omega)/\sigma_{DC} = i/(\omega + i\tau^{-1})$, against the frequency for varying the Fermi energy between 0.3 and 1.1 eV. Although at low doping concentration the THz response of graphene can be modeled with a Drude model with constant scattering time, at high doping levels, however, the scattering rate changes with the Fermi energy. The transport scattering time has two contributions associated with the long-range charge impurity scattering (τ_c) and short-range disorder scattering (τ_s) as $\tau^{-1} = \tau_c^{-1} + \tau_s^{-1}$.[26,36] These scattering mechanisms scale differently with the Fermi energy. For short-range scattering, the scattering rate is proportional to E_F; however, for long-range scattering,

DOI: 10.1021/acsphotonics.6b00240
ACS Photonics 2016, 3, 1531−1535

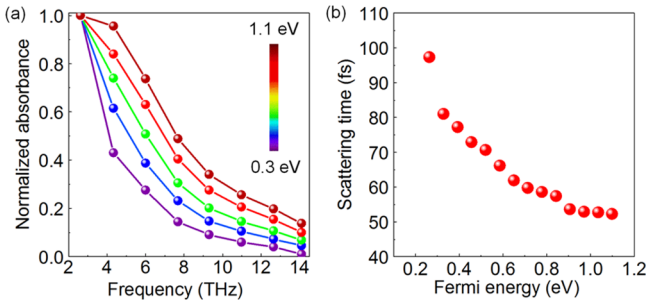

Figure 5. Drude response of graphene at high doping level. (a) Frequency dependence of the resonance absorbance at different Fermi energies. The absorbance is normalized by maximum absorbance at 2.8 THz. (b) Variation of the transport scattering time with the Fermi energy.

the scattering rate is inversely proportional to E_F. Our results show that, as the Fermi energy increases, the absorbance decays slower with increasing frequency, indicating a smaller scattering time. Using the Drude model, we extracted the Fermi energy dependence of the total scattering time (Figure 5b). Around the charge neutrality point, the scattering time is close to 100 fs and decreases down to 50 fs at Fermi energies of 1.1 eV.

To show the promises of our approach, we demonstrate flexible active THz surfaces as the application part of our work. The tunable coherent absorption of THz radiation can lead to new types of active THz devices. Conventional THz devices are rigid, which prevents realization of flexible THz components. The atomic thickness of graphene together with the simple device geometry allows us to fabricate a tunable THz cavity on a flexible polymer substrate. Figure 6a shows a photograph of

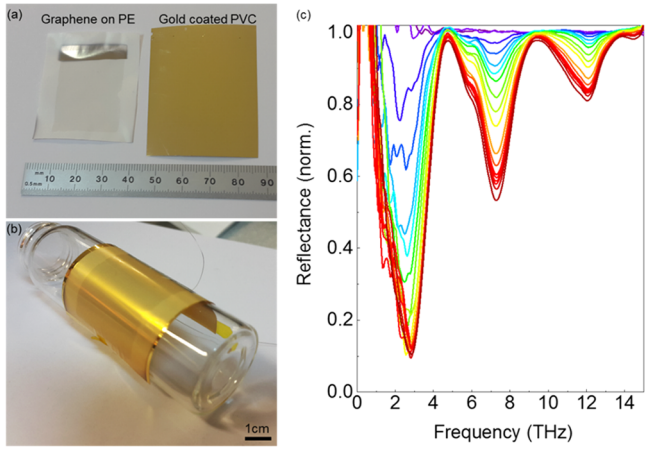

Figure 6. Flexible active THz surfaces. (a) Photograph of the large-area graphene on PE membrane and gold-coated PVC substrate. (b) Fabricated device rolled around a glass cylinder with a diameter of 2.7 cm. (c) THz reflectivity spectrum from the curved surface at different bias voltages.

large-area graphene (2.5 × 3.0 cm^2) on a porous PE membrane and gold-coated PVC substrate. After injecting an ionic liquid into the PE membrane (20 μm thick), we placed it on the gold-coated PVC substrate and rolled the device around a glass cylinder with a diameter of 2.7 cm (Figure 6b). We measured the variation of the THz reflectivity from the curved surface. During the measurement the beam size is set to 6 mm in diameter. Similar to the rigid devices, we observed three resonances, at 3, 7.2, and 12.2 THz (Figure 6c). The first resonance yields gate-tunable absorption up to 95% at 2 V bias voltage.

In conclusion, we report experimental observation of gate-tunable coherent perfect absorption of terahertz radiation in highly doped graphene. Our work has four novel parts. First, we developed an electrically tunable THz cavity using a THz transparent porous membrane soaked with an ionic liquid electrolyte sandwiched between graphene and gold electrodes. In this device geometry the gold electrode operates as both reflecting mirror and the gate electrode. Second, we observed the coherent perfect absorption of THz radiation in graphene. The ability to gate graphene up to 1 eV Fermi levels in the THz cavity allows us to observe a critical coupling condition that yields an absorption of 99%. Third, this novel device configuration allows direct measurement of the Fermi energy and elucidating the doping dependence of the transport scattering time, which varies from 100 fs down to 50 fs as the Fermi energy changes from 0.2 to 1.1 eV. Finally, using these structures we demonstrated flexible active THz surfaces with voltage-controlled THz reflectance. We anticipate that our work providing a developed device structure as a new platform to study gate-tunable CPA will lead to efficient active THz components such as tunable THz mirrors and modulators.

■ ASSOCIATED CONTENT

Supporting Information

The Supporting Information is available free of charge on the ACS Publications website at DOI: 10.1021/acsphotonics.6b00240.

Transmission line models for the freestanding graphene and the active device, THz transmittance of the PE membrane, voltage-controlled IR reflectivity from the device, variation of the center frequency and width of the resonance with the bias voltage, voltage-controlled reflectivity of the device characterized by 0.368 THz continuous THz source (PDF)

■ AUTHOR INFORMATION

Corresponding Author

*E-mail: ckocabas@fen.bilkent.edu.tr.

Notes

The authors declare no competing financial interest.

■ ACKNOWLEDGMENTS

This work was partially supported by the Scientific and Technological Research Council of Turkey (TUBITAK) grant no. 114F379 and the European Research Council (ERC) Consolidator Grant ERC-682723 SmartGraphene. N.K. acknowledges the TUBITAK-BIDEB 2215 scholarship program.

■ REFERENCES

(1) Chong, Y. D.; Ge, L.; Cao, H.; Stone, A. D. Coherent Perfect Absorbers: Time-Reversed Lasers. *Phys. Rev. Lett.* **2010**, *105*, 053901.

(2) Wan, W. Time-reversed lasing and interferometric control of absorption (vol 331, pg 889, 2011). *Science* **2011**, *334*, 1058−1058.

(3) Pu, M. B.; Feng, Q.; Wang, M.; Hu, C. G.; Huang, C.; Ma, X. L.; Zhao, Z. Y.; Wang, C. T.; Luo, X. G. Ultrathin broadband nearly perfect absorber with symmetrical coherent illumination. *Opt. Express* **2012**, *20*, 2246−2254.

(4) Feng, S.; Halterman, K. Coherent perfect absorption in epsilon-near-zero metamaterials. *Phys. Rev. B: Condens. Matter Mater. Phys.* **2012**, *86*, 165103.

DOI: 10.1021/acsphotonics.6b00240
ACS Photonics 2016, 3, 1531−1535

(5) Longhi, S. Coherent perfect absorption in a homogeneously broadened two-level medium. *Phys. Rev. A: At., Mol., Opt. Phys.* **2011**, *83*, 055804.
(6) Kats, M. A.; Sharma, D.; Lin, J.; Genevet, P.; Blanchard, R.; Yang, Z.; Qazilbash, M. M.; Basov, D. N.; Ramanathan, S.; Capasso, F. Ultra-thin perfect absorber employing a tunable phase change material. *Appl. Phys. Lett.* **2012**, *101*, 221101.
(7) Noh, H.; Chong, Y. D.; Stone, A. D.; Cao, H. Perfect coupling of light to surface plasmons by coherent absorption. *Phys. Rev. Lett.* **2012**, *108*, 186805.
(8) Balci, O.; Polat, E. O.; Kakenov, N.; Kocabas, C. Graphene-enabled electrically switchable radar-absorbing surfaces. *Nat. Commun.* **2015**, *6*, 6628.
(9) Wang, F.; Chen, C. F.; Park, C. H.; Boudouris, B. W.; Horng, J.; Geng, B. S.; Girit, C.; Zettl, A.; Crommie, M. F.; Segalman, R. A.; Louie, S. G. Controlling inelastic light scattering quantum pathways in graphene. *Nature* **2011**, *471*, 617−620.
(10) Zhang, X.; Liu, M.; Yin, X. B.; Ulin-Avila, E.; Geng, B. S.; Zentgraf, T.; Ju, L.; Wang, F. A graphene-based broadband optical modulator. *Nature* **2011**, *474*, 64−67.
(11) Wang, F.; Zhang, Y. B.; Tian, C. S.; Girit, C.; Zettl, A.; Crommie, M.; Shen, Y. R. Gate-variable optical transitions in graphene. *Science* **2008**, *320*, 206−209.
(12) Sensale-Rodriguez, B.; Yan, R. S.; Kelly, M. M.; Fang, T.; Tahy, K.; Hwang, W. S.; Jena, D.; Liu, L.; Xing, H. G. Broadband graphene terahertz modulators enabled by intraband transitions. *Nat. Commun.* **2012**, *3*, 780.
(13) Polat, E. O.; Kocabas, C. Broadband Optical Modulators Based on Graphene Supercapacitors. *Nano Lett.* **2013**, *13*, 5851−5857.
(14) Kakenov, N.; Balci, O.; Polat, E. O.; Altan, H.; Kocabas, C. Broadband terahertz modulators using self-gated graphene capacitors. *J. Opt. Soc. Am. B* **2015**, *32*, 1861−1866.
(15) Kakenov, N.; Takan, T.; Ozkan, V. A.; Balci, O.; Polat, E. O.; Altan, H.; Kocabas, C. Graphene-enabled electrically controlled terahertz spatial light modulators. *Opt. Lett.* **2015**, *40*, 1984−1987.
(16) Bosman, H.; Lau, Y. Y.; Gilgenbach, R. M. Microwave absorption on a thin film. *Appl. Phys. Lett.* **2003**, *82*, 1353−1355.
(17) Fang, Z. Y.; Wang, Y. M.; Schather, A. E.; Liu, Z.; Ajayan, P. M.; de Abajo, F. J. G.; Nordlander, P.; Zhu, X.; Halas, N. J. Active Tunable Absorption Enhancement with Graphene Nanodisk Arrays. *Nano Lett.* **2014**, *14*, 299−304.
(18) Majumdar, A.; Kim, J.; Vuckovic, J.; Wang, F. Electrical Control of Silicon Photonic Crystal Cavity by Graphene. *Nano Lett.* **2013**, *13*, 515−518.
(19) Engel, M.; Steiner, M.; Lombardo, A.; Ferrari, A. C.; Lohneysen, H. V.; Avouris, P.; Krupke, R. Light-matter interaction in a microcavity-controlled graphene transistor. *Nat. Commun.* **2012**, *3*, 906.
(20) Furchi, M.; Urich, A.; Pospischil, A.; Lilley, G.; Unterrainer, K.; Detz, H.; Klang, P.; Andrews, A. M.; Schrenk, W.; Strasser, G.; Mueller, T. Microcavity-Integrated Graphene Photodetector. *Nano Lett.* **2012**, *12*, 2773−2777.
(21) Thareja, V.; Kang, J. H.; Yuan, H. T.; Milaninia, K. M.; Hwang, H. Y.; Cui, Y.; Kik, P. G.; Brongersma, M. L. Electrically Tunable Coherent Optical Absorption in Graphene with Ion Gel. *Nano Lett.* **2015**, *15*, 1570−1576.
(22) Liu, Y. H.; Chadha, A.; Zhao, D. Y.; Piper, J. R.; Jia, Y. C.; Shuai, Y. C.; Menon, L.; Yang, H. J.; Ma, Z. Q.; Fan, S. H.; Xia, F. N.; Zhou, W. D. Approaching total absorption at near infrared in a large area monolayer graphene by critical coupling. *Appl. Phys. Lett.* **2014**, *105*, 181105.
(23) Woo, J. M.; Kim, M. S.; Kim, H. W.; Jang, J. H. Graphene based salisbury screen for terahertz absorber. *Appl. Phys. Lett.* **2014**, *104*, 081106.
(24) Thongrattanasiri, S.; Koppens, F. H. L.; de Abajo, F. J. G. Complete Optical Absorption in Periodically Patterned Graphene. *Phys. Rev. Lett.* **2012**, *108*, 047401.
(25) Zhang, J. F.; Guo, C. C.; Liu, K.; Zhu, Z. H.; Ye, W. M.; Yuan, X. D.; Qin, S. Q. Coherent perfect absorption and transparency in a nanostructured graphene film. *Opt. Express* **2014**, *22*, 12524−12532.
(26) Liu, F. L.; Chong, Y. D.; Adam, S.; Polini, M. Gate-tunable coherent perfect absorption of terahertz radiation in graphene. *2D Mater.* **2014**, *1*, 031001.
(27) Fan, Y. C.; Zhang, F. L.; Zhao, Q.; Wei, Z. Y.; Li, H. Q. Tunable terahertz coherent perfect absorption in a monolayer graphene. *Opt. Lett.* **2014**, *39*, 6269−6272.
(28) Li, S. C.; Duan, Q.; Li, S.; Yin, Q.; Lu, W. X.; Li, L.; Gu, B. M.; Hou, B.; Wen, W. J. Perfect electromagnetic absorption at one-atom-thick scale. *Appl. Phys. Lett.* **2015**, *107*, 181112.
(29) Pirruccio, G.; Moreno, L. M.; Lozano, G.; Rivas, J. G. Coherent and Broadband Enhanced Optical Absorption in Graphene. *ACS Nano* **2013**, *7*, 4810−4817.
(30) Rao, S. M.; Heitz, J. J. F.; Roger, T.; Westerberg, N.; Faccio, D. Coherent control of light interaction with graphene. *Opt. Lett.* **2014**, *39*, 5345−5347.
(31) Sensale-Rodriguez, B.; Yan, R. S.; Liu, L.; Jena, D.; Xing, H. G. Graphene for Reconfigurable Terahertz Optoelectronics. *Proc. IEEE* **2013**, *101*, 1705−1716.
(32) Kakenov, N.; Balci, O.; Polat, E. O.; Altan, H.; Kocabas, C. Broadband terahertz modulators using self-gated graphene capacitors. *J. Opt. Soc. Am. B* **2015**, *32*, 2548−2548.
(33) Brida, D.; Tomadin, A.; Manzoni, C.; Kim, Y. J.; Lombardo, A.; Milana, S.; Nair, R. R.; Novoselov, K. S.; Ferrari, A. C.; Cerullo, G.; Polini, M. Ultrafast collinear scattering and carrier multiplication in graphene. *Nat. Commun.* **2013**, *4*, 1987.
(34) Shi, S. F.; Tang, T. T.; Zeng, B.; Ju, L.; Zhou, Q.; Zettl, A.; Wang, F. Controlling Graphene Ultrafast Hot Carrier Response from Metal-like to Semiconductor-like by Electrostatic Gating. *Nano Lett.* **2014**, *14*, 1578−1582.
(35) Frenzel, A. J.; Lui, C. H.; Shin, Y. C.; Kong, J.; Gedik, N. Semiconducting-to-Metallic Photoconductivity Crossover and Temperature-Dependent Drude Weight in Graphene. *Phys. Rev. Lett.* **2014**, *113*, 056602.
(36) Adam, S.; Hwang, E. H.; Galitski, V. M.; Das Sarma, S. A self-consistent theory for graphene transport. *Proc. Natl. Acad. Sci. U. S. A.* **2007**, *104*, 18392−18397.

DOI: 10.1021/acsphotonics.6b00240
ACS Photonics 2016, 3, 1531−1535